Sensorless Field Oriented Control of PMSM drives based on Full Order SMO

Oussama Saadaoui, Amor Khlaief, Moez Abassi, Abdelkader Chaari, Mohamed Boussak

Sensorless FOC of PMSM drives based on Full Order SMO

O. Saadaoui, A. Khlaief, M. Abassi, A. Chaari
Laboratoire d'Ingénierie des Systèmes Industriels et des Energies Renouvelables (LISIER)
Ecole Nationale Supérieure d'Ingénieurs de Tunis
(e-mail: saadaoui.oussama1@gmail.com, abdelkader.chaari@ensit.rnu.tn).

M. Boussak
Laboratoire des Sciences de l'Information et des Systèmes
Ecole Centrale Marseille– France
e-mail: mohamed.boussak@centrale-marseille.fr.

***Abstract*—This document deals with a sensorless field oriented control (FOC) for permanent magnet synchronous motor (PMSM) drives by using a full order sliding mode observer (FOSMO). We have constructed a FO-SMO to estimate the position and velocity. The Lyapunov theorem is used to verify the FO-SMO stability. The experimental findings indicate the robustness of SM observer under parametric variations.**

Keywords— Digital signal processor, FO-SMO, PMSM, Sensorless, Sign function.

I. Introduction

The synchronous permanent magnet motors (PMSM) are spreading more and more as actuators in high performance industry applications owing to their reliable performance, high effiency, good controllability, high power density and relatively low cost, [1]. Nowadays the PMSM are used in paper mills, wind energy, variable speed elevators, drives for ships, aircraft actuators. Vector control needs always complete information of position and angular speed measured by an encoder or a resolver sensor. This mechanical sensor given various drawbacks due to additional cost, additional electronic circuit for processing information and more cables. For the reason, during the last twenty years, several researches have been developed sensorless PMSM drives strategies [2]–[4] in order to remove the mechanical sensor.

Most of these strategies have been applied to estimate the speed and rotor position using the nonlinear observer [10], MRAS technique [4], the SM observer [7], an extended state observer [5] and an EKF [6]. Several researchers apply the SM observer method in order to detect the velocity/position of the motor; which characterized by its robustness versus parametric variations.

In [8], the researchers present a new SM observer of the PM synchronous motor where they substitute the sign function by another function which called sigmoid function to decrease the chattering phenomenon.

In [9], the authors estimated the rotor speed/position for PM synchronous motor with initial rotor position detection.

Consequently, this document is composed of 5 parts: part 2 shows the PMSM model, the SM observer design is given by part 3, part 4 is reserved for the experimental findings, and section 5 shows the parameter perturbation robustness analysis.

II. PMSM Model

The PM synchronous motor model is given by:

$$\begin{cases} \dfrac{di_\alpha}{dt} = -\dfrac{R_s}{L_s} i_\alpha + \dfrac{n_p K_e}{L_s} \Omega_r \sin(\theta_r) + \dfrac{1}{L_s} V_\alpha \\ \dfrac{di_\beta}{dt} = -\dfrac{R_s}{L_s} i_\beta + \dfrac{n_p K_e}{L_s} \Omega_r \cos(\theta_r) + \dfrac{1}{L_s} V_\beta \\ \dfrac{d\Omega_r}{dt} = \dfrac{n_p K_e}{J} \left(i_\beta \cos(\theta_r) - i_\alpha \sin(\theta_r) \right) - \dfrac{f}{J} \Omega_r \\ \dfrac{d\theta_r}{dt} = \Omega_r \end{cases} \quad (1)$$

with

$i_{\alpha,\beta}$: Phase currents.
$V_{\alpha,\beta}$: Voltage of $\alpha - \beta$ axis.
R_s : Resistance.
L_s : Inductance.
K_e : Electromotive force.
Ω_r : Mechanical speed.
θ_r : Electrical rotor position.
n_p : Number of pole pairs.

III. SMO Design

A. SM observer

Most Based on PMSM model (1), the full-order sliding mode observer (FO-SMO) is expressed as:

$$\begin{cases} \dfrac{d\hat{i}_\alpha}{dt} = -\dfrac{R_s}{L_s}\hat{i}_\alpha + \dfrac{n_p K_e}{L_s}\hat{\Omega}\sin(\hat{\theta}) + \dfrac{1}{L_s}V_\alpha + k_1\,\mathrm{sgn}(i_\alpha - \hat{i}_\alpha) \\ \dfrac{d\hat{i}_\beta}{dt} = -\dfrac{R_s}{L_s}\hat{i}_\beta + \dfrac{n_p K_e}{L_s}\hat{\Omega}\cos(\hat{\theta}) + \dfrac{1}{L_s}V_\beta + k_1\,\mathrm{sgn}(i_\beta - \hat{i}_\beta) \\ \dfrac{d\hat{\Omega}}{dt} = \dfrac{n_p K_e}{J}\left(\hat{i}_\beta\cos(\hat{\theta}) - \hat{i}_\alpha\sin(\hat{\theta})\right) - \dfrac{f}{J}\hat{\Omega} + k_2\,\mathrm{sgn}(i_\alpha - \hat{i}_\alpha) + k_2\,\mathrm{sgn}(i_\beta - \hat{i}_\beta) \\ \dfrac{d\hat{\theta}}{dt} = \hat{\Omega} + k_3\,\mathrm{sgn}(i_\alpha - \hat{i}_\alpha) + k_3\,\mathrm{sgn}(i_\beta - \hat{i}_\beta) \end{cases} \quad (2)$$

with k_1, k_2 and k_3 are constant gains and $\mathrm{sgn}(\hat{i}_\alpha - i_\alpha)$ is the switching function.

The model (2) shows the SMO where the signum function is apply as the switching function. In order to eliminate the chattering phenomenon, we used a low pass filter (LPF) from the switching.

B. Stability analysis

We have selected the sliding surface as follows

$$S(x) = \left[S_\alpha(\mathrm{x})\; S_\beta(x)\right]^T = \begin{bmatrix} \hat{i}_\alpha - i_\alpha \\ \hat{i}_\beta - i_\beta \end{bmatrix} \quad (3)$$

We choose the Lyapunov function as

$$\begin{aligned} V &= \frac{1}{2}\left(S_\alpha{}^2 + S_\beta{}^2 + \bar{\Omega}^2 + \bar{\theta}^2\right) \\ &= \frac{1}{2}\left(\bar{i}_\alpha{}^2 + \bar{i}_\beta{}^2 + \bar{\Omega}^2 + \bar{\theta}^2\right) \end{aligned} \quad (4)$$

with $\bar{i}_\alpha = i_\alpha - \hat{i}_\alpha, \bar{i}_\beta = i_\beta - \hat{i}_\beta, \bar{\Omega} = \Omega - \hat{\Omega}$ and $\bar{\theta} = \theta - \hat{\theta}$.

Its derivative

$$\frac{dV}{dt} = \bar{i}_\alpha\frac{d\bar{i}_\alpha}{dt} + \bar{i}_\beta\frac{d\bar{i}_\beta}{dt} + \bar{\Omega}_r\frac{d\bar{\Omega}_r}{dt} + \bar{\theta}_r\frac{d\bar{\theta}_r}{dt} \quad (5)$$

The dynamic errors equations are presented as follows:

$$\begin{cases} \dot{\bar{i}}_\alpha = -\dfrac{R_s}{L_s}\bar{i}_\alpha + \dfrac{n_p K_e}{L_s}\left(\Omega_r\sin\theta_r - \hat{\Omega}_r\sin\hat{\theta}_r\right) - k_1\,\mathrm{sgn}(\bar{i}_\alpha) \\ \dot{\bar{i}}_\beta = -\dfrac{R_s}{L_s}\bar{i}_\beta + \dfrac{n_p K_e}{L_s}\left(-\Omega_r\cos\theta_r + \hat{\Omega}_r\cos\hat{\theta}_r\right) - k_1\,\mathrm{sgn}(\bar{i}_\beta) \\ \dot{\bar{\Omega}}_r = \dfrac{n_p K_e}{J}\left(i_\beta\cos\theta_r - i_\alpha\sin\theta_r\right) - \left(\hat{i}_\beta\cos\hat{\theta}_r - \hat{i}_\alpha\sin\hat{\theta}_r\right) - \dfrac{f}{J}\bar{\Omega}_r - k_2\,\mathrm{sgn}(\bar{i}_\alpha) - k_2\,\mathrm{sgn}(\bar{i}_\beta) \\ \dot{\bar{\theta}}_r = \Omega_r - \hat{\Omega}_r - k_3\,\mathrm{sgn}(\bar{i}_\alpha) - k_3\,\mathrm{sgn}(\bar{i}_\beta) \end{cases} \quad (6)$$

By substituting (6) in (5), we obtain

$$\begin{aligned} \dot{V} = &-a_1\bar{i}_\alpha{}^2 + a_2\bar{i}_\alpha\left(\Omega_r\sin\theta_r - \hat{\Omega}_r\sin\hat{\theta}_r\right) - K_1\left|\bar{i}_\alpha\right| \\ &- a_1\bar{i}_\beta{}^2 + a_2\bar{i}_\beta\left(\Omega_r\cos\theta_r - \hat{\Omega}_r\cos\hat{\theta}_r\right) - K_1\left|\bar{i}_\beta\right| - a_4\bar{\Omega}_r{}^2 \\ &+ a_3\bar{\Omega}_r\left[(i_\beta\cos\theta_r - i_\alpha\sin\theta_r) - (\hat{i}_\beta\cos\hat{\theta}_r - \hat{i}_\alpha\sin\hat{\theta}_r)\right] \\ &- \bar{\Omega}_r K_2\mathrm{sgn}(\bar{i}_\alpha) - \bar{\Omega}_r K_2\mathrm{sgn}(\bar{i}_\beta) + \bar{\theta}_r\,\bar{\Omega}_r - \bar{\theta}_r K_3\mathrm{sgn}(\bar{i}_\alpha) \\ &- \bar{\theta}_r K_3\mathrm{sgn}(\bar{i}_\beta) \end{aligned} \quad (7)$$

with

$$\begin{cases} a_1 = \dfrac{R_S}{L_S},\; a_2 = \dfrac{n_p K_e}{L_S},\; a_3 = \dfrac{n_p K_e}{J},\; a_4 = \dfrac{f}{J} \\ \left|\bar{i}_\alpha\right| = i_\alpha\,\mathrm{sgn}\left(\bar{i}_\alpha\right) \\ \left|\bar{i}_\beta\right| = i_\beta\,\mathrm{sgn}\left(\bar{i}_\beta\right) \end{cases} \quad (8)$$

In order to ensure the convergence, the derivative (5) is forced such that $\dot{V} < 0$.

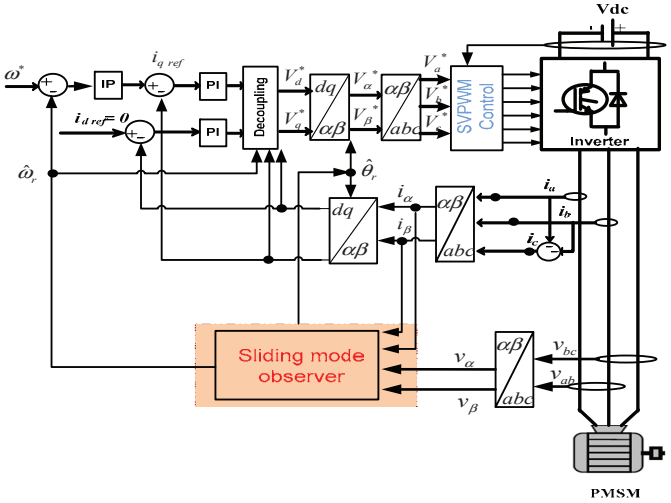

(a)

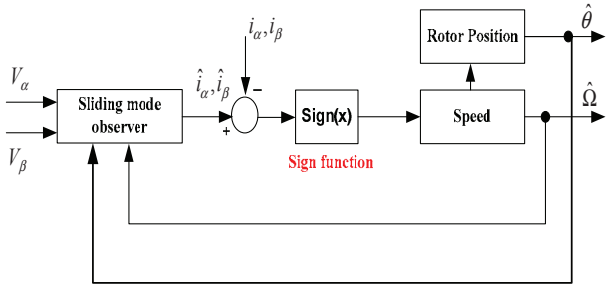

(b)

Fig. 1. Diagram of the sensorless FO control of PM synchronous motor. (a) System overview. (b) SM observer presentation.

Knowing that

$$\begin{cases} -a_1\bar{i}_\alpha{}^2 < 0,\; -a_1\bar{i}_\beta{}^2 < 0,\; -a_4\bar{\Omega}_r{}^2 < 0 \\ \left|\Omega_r\sin\theta_r - \hat{\Omega}_r\sin\hat{\theta}_r\right| < 2\Omega_{\max} \\ \left|\bar{i}_\alpha(\Omega_r\sin\theta_r - \hat{\Omega}_r\sin\hat{\theta}_r)\right| < 4i_{\max}\Omega_{\max} \end{cases} \quad (9)$$

Such that

$$\begin{cases} \left|\bar{i}_\alpha\right| < 2i_{\max} \\ \left|\bar{i}_\beta\right| < 2i_{\max} \end{cases} \quad (10)$$

Therefore

$$\begin{cases} \left|\bar{i}_{\alpha,\beta}(\Omega_r \sin\theta_r - \hat{\Omega}_r \sin\hat{\theta}_r)\right| < 4 i_{\max}\Omega_{\max} \\ \left|\bar{i}_{\beta}(\Omega_r \cos\theta_r - \hat{\Omega}_r \cos\hat{\theta}_r)\right| < 4 i_{\max}\Omega_{\max} \\ \left|\bar{\Omega}_r\left[(i_\beta \cos\theta_r - i_\alpha \sin\hat{\theta}_r) - (\hat{i}_\beta \cos\hat{\theta}_r - \hat{i}_\alpha \sin\hat{\theta}_r)\right]\right| < 8 i_{\max}\Omega_{\max} \\ \left|\bar{\theta}_r \bar{\Omega}_r\right| < 4\theta_{\max}\Omega_{\max} \\ \left|\bar{\Omega}_r(\mathrm{sgn}(\bar{i}_\alpha) + \mathrm{sgn}(\bar{i}_\beta))\right| < 4\Omega_{\max} \end{cases} \quad (11)$$

We select k_1, k_2 and k_3 as

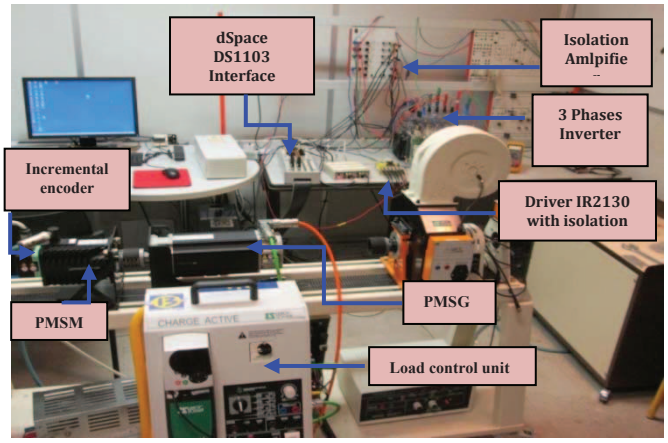

Fig. 2. Test bench for PMSM electric-drive machine.

$$\begin{aligned} & a_2\bar{i}_\alpha\left(\Omega_r \sin\theta_r - \hat{\Omega}_r \sin\hat{\theta}_r\right) + a_2\bar{i}_\beta\left(\Omega_r \cos\theta_r - \hat{\Omega}_r \cos\hat{\theta}_r\right) \\ & + a_3\bar{\Omega}_r\left[(i_\beta \cos\theta_r - i_\alpha \sin\hat{\theta}_r) - (\hat{i}_\beta \cos\hat{\theta}_r - \hat{i}_\alpha \sin\hat{\theta}_r)\right] \\ & - k_1\left|\bar{i}_\alpha\right| - k_1\left|\bar{i}_\beta\right| - \bar{\Omega}_r K_2 \mathrm{sgn}(\bar{i}_\alpha) - \bar{\Omega}_r k_2 \mathrm{sgn}(\bar{i}_\beta) + \bar{\theta}_r\ \bar{\Omega}_r \\ & - \bar{\theta}_r k_3 \mathrm{sgn}(\bar{i}_\alpha) - \bar{\theta}_r k_3 \mathrm{sgn}(\bar{i}_\beta) < 0 \end{aligned} \quad (12)$$

As a result,

$$k_1 > 2a_2\Omega_{\max},\ \ k_2 > 2a_3 i_{\max} \text{ and } k_3 > \Omega_{\max} \quad (13)$$

Fig. 1 gives the layout of sensorless FO control of the PM synchronous motor. We apply $u_{\alpha,\beta}$ and $i_{\alpha,\beta}$ as an inputs voltages and currents, respectively of our observer.

IV. Experimental Results

To validate the feasibility of the approach, an experimental platform is built (see Fig. 2). The parameters values of PM synchronous motor are indicated in Table I.

A. Simulation results

Figure 3 displays the simulation results of the sensorless FOC based on the sign function. Figure 3(a) shows the estimated rotor velocity that managed to follow the measured value at a cycle speed to 90 rad/s until it returns to the stop state at time t = 1.2s, figure 3(b) gives the error speed.

This results obtained displays that the estimated and measured speed are identical during the operation; where the estimation error do not exceed 0.13 rad.

We can notice that measured and estimated position responses are corresponding where the error estimation do not exceed 4.510^{-2} rad (as represented in figure 3(d)).

B. Experimental results

Figure 4 displays the results for sensorless FOC based on sign function. As illustrated in Fig. 4, we observe that the measured and estimated speed and position responses are identical. As shown by the Fig. 4(b), the speed estimation error does not reach than 37 rpm in the course of the transient state.

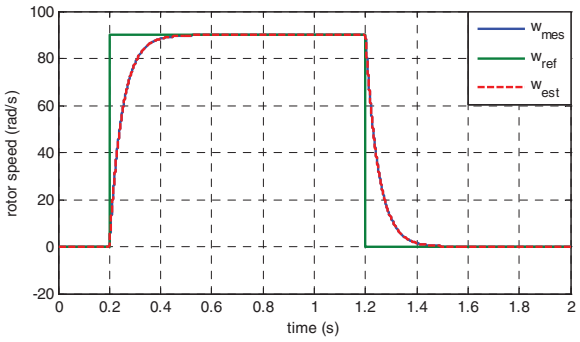

(a) Measured and estimated speed

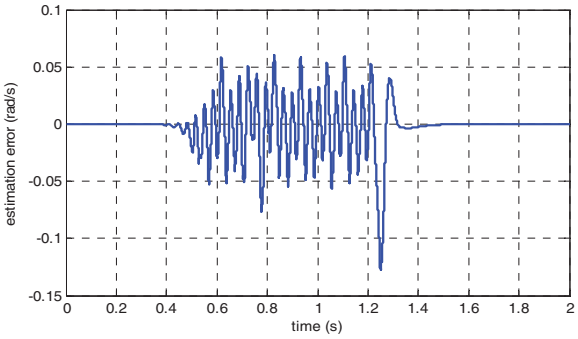

(b) Speed estimation error

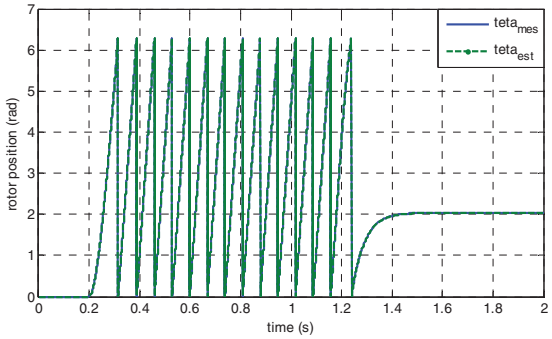

(c) Estimated and measured position

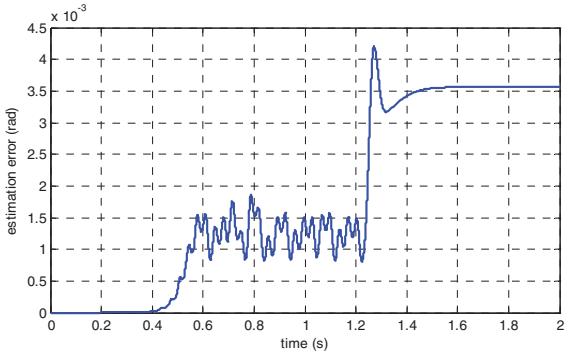

(d) Position estimation error

Fig. 3. Sensorless FOC based on the sign function

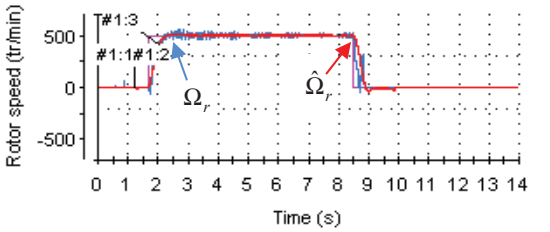

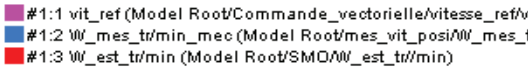

a) Measured and estimated speed

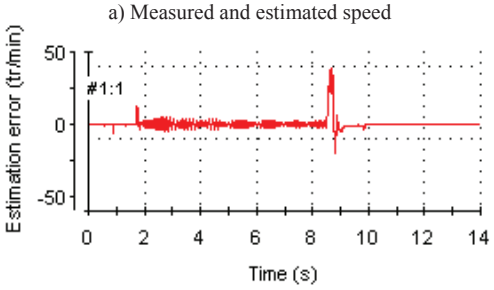

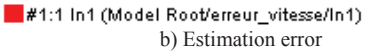

b) Estimation error

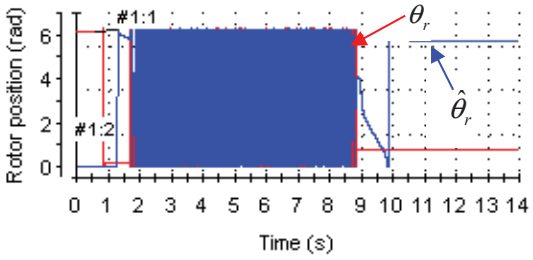

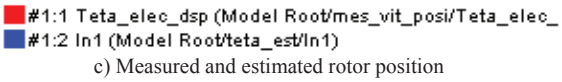

c) Measured and estimated rotor position

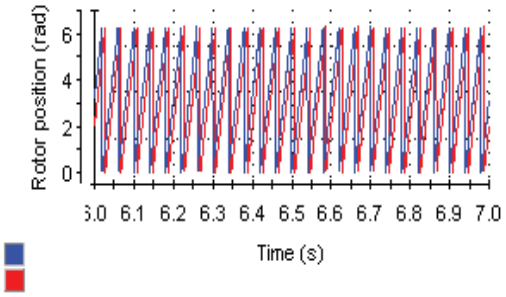

d) Zoomed in-view

V. Robustness Against Stator Resistance Variation

Robustness against parameter variations is an important criterion in order to assess speed regulator performance. During the operation of PM synchronous motor, the parameters of the motor are changing.

Fig. 4(c, d) shows the waveforms of estimated and measured rotor position. Fig. 4(e) given the zoomed estimated and measured current of α -axis.

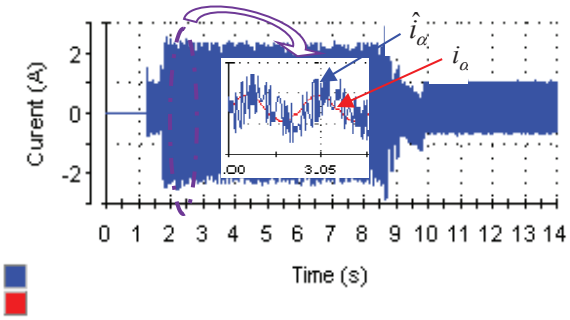

e) zoomed i_α and $\hat{i}_\alpha$

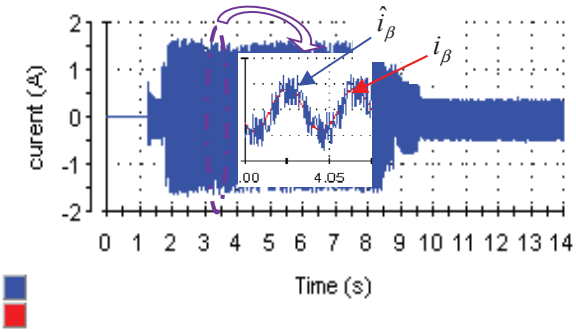

f) zoomed i_β and $\hat{i}_\beta$

Fig. 4. Experimental results with a variation speed from 500 rpm to 0 rpm using the sign function

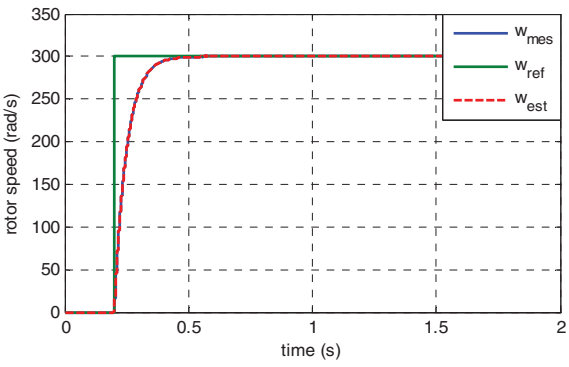

a) speed dynamics (R_s)

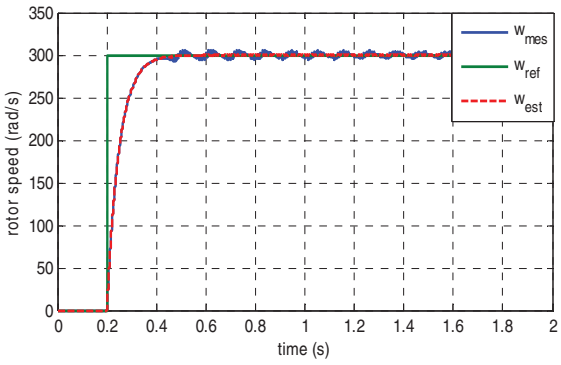

b) speed dynamics (+20% of R_s)

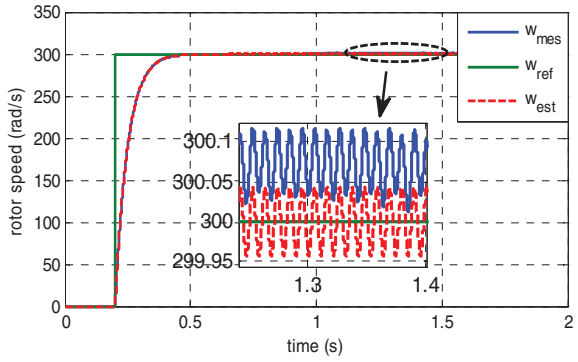

c) speed dynamics (-10% of R_s)

Fig. 5. speed dynamics during stator resistance variations.

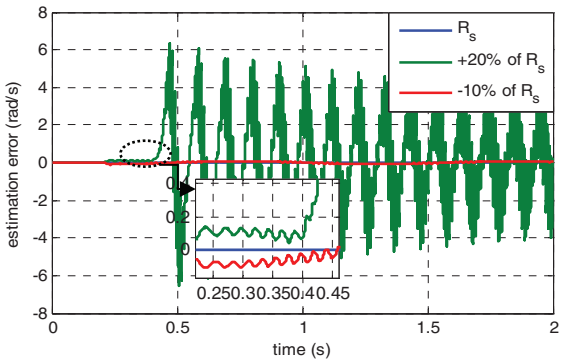

Fig. 6. Error estimation

Fig. 4 (f) exhibits the zoomed current of β -axis. The use of sign function which requires a LPF leads to appear fluctuations in stator currents (see Fig 4(e, f)).

We observe that the estimation errors of the velocity and rotor position are weak and which validate the robustness of the SM observer.

When the rotor speed keeps its good performance during operation against the parametric variations, so we can conclude that the speed regulator is more robust. In the case of application a changes for the stator resistance, the follows section gives the simulation results obtained of the sensorless FOC for PMSM.

Fig. 5 displays the results obtained to change the stator resistance during PMSM operation. The rotor speed response is practically unchanged in the case where the stator resistance equal -10% of the nominal value. In the case the resistance present +20 % of the nominal value, rotor speed response oscillates slightly during the steady state.

From Fig. 6, we observe that the speed estimation error achieved 6 rad/s in the case where stator resistance multiplied by 1.2. In fact, the proposed FOC exhibits a good robustness versus of the R_s parameter variation.

These simulation results indicate that field oriented control has good robustness versus perturbation.

VI. Conclusion

The capacity of sensorless FOC of PM synchronous motor drives based on FO SM observer was investigated in our work. The observer stability has been proved by using the Lyapunov function.

The findings have demonstrated the efficiency of sensorless field oriented control of the PM synchronous motor drives. With these results, we check the effectiveness of the sensorless control versus parametric variations.

In the next phases, we find it interesting to make ameliorations of our technique for salient-PMSM drive.

Appendix

Table I. Motor parameter

Constant parameter		Control parameter	
Rated speed	3000 rpm	Number of pole pairs	3
Inertia	0.0036 Kg.m^2	Rated power	1.1 kW
Stator resistance	6.2 Ω	IP speed regulator	$K_{p\_\Omega}=15,\ K_{i\_\Omega}=6$
d-axis stator inductance	$L_d=25.025$ mH	PI currents controller	$K_{p\_id}=2200, K_{i\_id}=40;$ $K_{p\_iq}=400, K_{i\_iq}=40$
q-axis stator inductance	$L_q=40.17$ mH	SMO gain	$K_1=10000$ $K_2=25, K_3=8$
Rated load torque	4 Nm		
Friction coefficient	0.0011 Nm/rad/s		
Torque constant	0.9149 Nm/A		

References

[1] B. Alecsa, M. N. Cirstea and A. Onea, "Simulink modeling and design of an efficient hardware-constrained FPGA-based PMSM speed controller," *IEEE Transactions on Industrial Informatics*, vol. 8, pp. 554–562, 2012.

[2] R. Wu and G. R. Selmon, "A permanent magnet motor drive without a shaft sensor," *IEEE Transactions Industry Applications*, vol. 27, pp. 1005–1011, 1991.

[3] S. Chi, Z. Zhang and L. Xu, "Sliding-mode sensorless control of direct drive PM synchronous motors for washing machine applications," *IEEE Transactions Industry Applications*, vol. 45, pp. 582–590, 2009.

[4] D. M. Lee, "On-line parameter identification of SPM motors based on MRAS technique," *International Journal of Electronics*, DOI: 10.1080/00207217.2016.1220635, 2016.

[5] H. Liu and S. Li, "Speed control for PMSM servo system using predictive functional control and extended state observer," *IEEE Transactions Industrial Electronics*, vol. 59, pp. 1171–1183, 2012.

[6] K. Q. Nguyen, D. T. Doan and Q. P. Ha, "FPGA-based sensorless PMSM speed control using adaptive extended kalman filter," *International Conf. on Automation Science and Engineering (CASE)*, pp. 1650–1655, 2015.

[7] O. Saadaoui, A. Khlaief, A. Chaari and M. Boussak, "A new approach rotor speed estimation for PMSM based on sliding mode observer", *Journal of Automation & Systems Engineering*, vol. 9, pp. 66–78, 2015.

[8] O. Saadaoui, A. Khlaief, M. Abassi, A. Chaari and M. Boussak, "Position sensorless vector control of PMSM drives based on SMO,"

International Conference on Sciences and Techniques of Automatic Control and Computer Engineering, 545–550, 2015.

[9] O. Saadaoui, A. Khlaief, M. Abassi, A. Chaari and M. Boussak, "A sliding mode observer for high-performance sensorless control of PMSM with initial rotor position detection," *International Journal of Control (IJC),* DOI: 10.1080/00207179.2016.1181788, 2016.

[10] A. Khlaief, O. Saadaoui, M. Boussak, A. Chaari, "Implementation of stator resistance adaptation for sensorless speed control of IPMSM drive based on nonlinear position observer ," *International Conference on Electrical Machines,* pp. 1071–1077, DOI: 10.1109/ICELMACH.2016.7732658, 2016.